Chinese Journal of Polymer Science Vol. 31, No. 12, (2013), 1685−1696

Chinese Journal of Polymer Science

HYDROGEN-BONDING INDUCED CHANGE OF CRYSTALLIZATION BEHAVIOR OF POLY(BUTYLENE SUCCINATE) IN ITS MIXTURES WITH BISPHENOL A*

Fa-liang Luo[a, b, c**], Fa-hai Luo[a, b], Qian Xing[c], Xiu-qin Zhang[c], Hong-qiao Jiao[d], Min Yao[d], Chun-tao Luo[d] and Du-jin Wang[c**]

[a] *Key Laboratory of Energy Resource and Chemical Engineering of Ningxia, Ningxia University, Yinchuan 750021, China*
[b] *Liupanshan High School of Ningxia, Yinchuan 750002, China*
[c] *Beijing National Laboratory for Molecular Sciences, CAS Key Laboratory of Engineering Plastics, Institute of Chemistry, Chinese Academy of Sciences, Beijing 100190, China*
[d] *Shenhua Ningxia Coal Industry Group, Yinchuan 750011, China*

Abstract In the present work, the blend of poly(butylene succinate) (PBS) and bisphenol A (BPA) was prepared by solution mixing, and the intermolecular interactions between the two components were characterized by a combination of nuclear magnetic resonance (NMR) and Fourier transform infrared spectroscopy (FTIR). The results showed that intermolecular hydrogen-bonding forms between the carbonyl group of PBS and phenol hydroxyl of BPA. With the increase of BPA content, more hydrogen bonds were formed. The effect of hydrogen bonding on the crystallization behavior of PBS was investigated by differential scanning calorimetry (DSC) and polarized optical microscopy (POM). The results showed that the overall isothermal crystallization kinetics and the spherulite growth rate of PBS decrease with the increase of BPA content, while the PBS spherulite size increases with BPA content.

Keywords: Poly(butylene succinate); Bisphenol A; Hydrogen bonding; Crystallization behavior.

INTRODUCTION

Poly(butylene succinate) (PBS), a typical synthetic biodegradable polymer with the advantages of good thermal stability, satisfactory mechanical properties and environmental friendliness, can be processed facilely to various products by traditional polymer processing methods such as injection molding, film-blowing and extrusion[1, 2]. In certain practical applications, however, PBS suffers from some limitations such as brittleness caused by its high crystalline properties. A simple modification method involves the blending of PBS with other polymers and additives. For example, a series of polymers have been blended with PBS and the crystallization behavior of the mixtures has been studied[3–16]. Inorganic fillers such as layered silicate and multiwalled carbon nanotubes were also used to improve the mechanical and thermal properties of PBS[17–21].

Generally, in addition to the inorganic additives, some low molecular weight organic substances are also added into polymer materials to improve their processibility and serving properties. For example, diphenyl phthalate is often added into polyvinyl chloride (PVC) as plasticizer to modify its processibility[22]. Some specific low molecular weight organic substances can greatly improve the thermal and mechanical properties of

* This work was supported by the National Natural Science Foundation of China (Nos. 51063004, 21264012) and China National Funds for Distinguished Young Scientists (No. 50925313).
** Corresponding authors: Fa-liang Luo (罗发亮), E-mail: flluo@iccas.ac.cn
Du-jin Wang (王笃金), E-mail: djwang@iccas.ac.cn
Received January 7, 2013; Revised February 6, 2013; Accepted February 21, 2013
doi: 10.1007/s10118-013-1364-y

some polymers by forming supramolecular structures. In our previous researches[23–26], stearic acid, used as an ordinary lubricant in polymer processing[22], was added into poly(ethylenimine) (PEI) or poly(propylene carbonate) (PPC), and specific non-covalent interactions of hydrogen bonding were formed, leading to the formation of supermolecular thermotropic smectic phase[24–26]. Additionally, the formed supramolecular structure was found to endow the PPC with satisfactory processibility and thermal stability[24]. Phenol compounds, employed as antioxidants in polymer processing[22], also have the potential to form strong intermolecular interaction by hydrogen bonding with polymers containing carbonyl, ether, or other functional groups, resulting in the improvement of polymer properties. Wu found that the addition of dihydric phenol can greatly improve the damping properties of polymer materials[27]. It was also reported that 4,4′-thiodipheol is effective for the modification of the thermal and mechanical properties of polyesters[28, 29]. Bisphenol A (BPA), 2,2-bis (4-hydroxyphenyl) propane, is usually added into plastics and oil paint as an antioxidant and thermal stabilizer[22]. As an important dihydric phenol, BPA has the potential to form specific interaction of hydrogen bonding with some polymers containing carbonyl or ether groups. Fei *et al*. investigated the blending system of BPA and poly(3-hydroxybutyrate-*co*-3-hydroxyvalerate) (PHBV), and found that the hydrogen-bonding interaction between the hydroxyl group of BPA and the ester group of PHBV can improve the break elongation of PHBV[30]. In the present work, BPA was used as a low molecular weight organic modifier to blend with PBS. The intermolecular interaction and crystallization behavior of the PBS/BPA mixtures were systematically investigated by a combination of nuclear magnetic resonance (NMR), Fourier transform infrared spectroscopy (FTIR), differential scanning calorimetry (DSC), polarized optical microscopy (POM) and wide angle X-ray diffraction (WAXD). Based on the experimental results, a schematic model was proposed to illustrate the interaction in the BPA/PBS mixtures.

EXPERIMENTAL

Materials and Mixture Preparation

PBS (M_w = 1.15 × 10^5, M_n = 8.01 × 10^4, PDI = 1.44) was supplied by Haier KeHua National Engineering Research Center of Plastics Co., Ltd. BPA was purchased from Beijing Chemical Plant (chemical purity grade). The chain structure of PBS and the molecular structure of BPA are shown below.

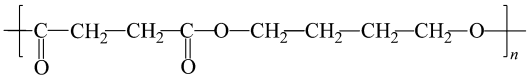

Chain structure of PBS

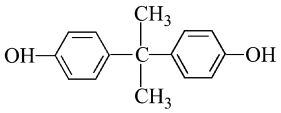

Molecular structure of BPA

The PBS/BPA mixtures with different compositions in weight ratio were prepared by solution casting. As the first step in the solution mixing process, 5 g samples of PBS and BPA weighed at a predesigned weight ratio were co-dissolved in 200 mL chloroform under 55 °C and stirred for 4 h. Then the solution was cast on a Petri dish, and the solvent was allowed to evaporate in the atmosphere. Finally, the blending film was dried in a vacuum oven at 50 °C for 58 h.

Nuclear Magnetic Resonance ^{1}H Spectroscopy (^{1}H-NMR)

High-resolution ^{1}H-NMR experiments were recorded at 400 MHz on a Bruker AV400 spectrometer. The solvent used was $CDCl_3$, and the concentration of the solution was controlled below 2% (g/mL). Tetramethylsilane was used as the internal standard.

Fourier Transform Infrared Spectroscopy (FTIR)

FTIR spectra were recorded on a Bruker EQUINOX 55 spectrometer at a resolution of 2 cm^{-1} with an accumulation of 32 scans. Samples for FTIR analysis were prepared by solution casting on the surface of a KBr crystal, followed by drying under infrared light to evaporate the residual solvent.

Differential Scanning Calorimetry (DSC)

The crystallization behavior of the PBS/BPA mixtures was studied under N_2 ambience with a Perkin-Elmer differential scanning calorimeter (DSC-7). The calibration for temperature and melting enthalpy was performed by using indium as the standard. Approximately 2–3 mg of the sample was sealed in aluminum pans and used for measurements. For the non-isothermal crystallization and the subsequent heating process, the samples were first heated to 200 °C and held for 5 min to erase the thermal history, then cooled to −40 °C at a cooling rate of 20 K/min. The subsequent heating process was executed at a heating rate of 20 K/min. For the isothermal crystallization process, the samples were first heated to 200 °C and held for 5 min to erase the thermal history, followed by rapid cooling to the crystallization temperature (T_c) at a maximum cooling rate of 150 K/min.

A Perkin-Elmer diamond differential scanning calorimeter, equipped with a liquid nitrogen cooling device, was used to detect the glass-transition temperature (T_g) of the samples. Approximately 5–6 mg of the samples was sealed in aluminum pans and used for measurements. The sample was first heated to 200 °C and held for 5 min to eliminate any thermal and mechanical history, then rapidly cooled to −100 °C at a maximum cooling rate of 200 K/min and kept for 10 min, and it was then heated to 200 °C at a heating rate of 20 K/min.

Polarized Optical Microscopy (POM)

The spherulite growth rates and morphology were determined by using an Olympus BX51 optical microscope, equipped with a Linkam THMS 600 thermal stage. Films with thickness of approximately 20 μm were sandwiched between two microscope cover glasses, melted at 200 °C for 5 min to erase the thermal history, and finally cooled to the preset temperature at a rate of 100 K/min for isothermal crystallization. The films for POM analysis were prepared by the solution casting method.

Wide Angle X-ray Diffraction (WAXD)

The WAXD measurements were performed at room temperature on a Rigaku model D/max-2B diffractometer using CuK_α radiation (λ = 0.154 nm). The measurements were operated at 40 kV and 200 mA. The samples for WAXD analysis were the dried films as mentioned in the experimental section.

RESULTS AND DISCUSSION

Interactions between PBS and BPA

NMR is a powerful technique to investigate the intermolecular and intramolecular interactions of organic small molecules or small molecule-macromolecule pairs. To elucidate the specific hydrogen-bonding interaction in the PBS/BPA mixtures by NMR, samples of pure PBS, BPA and PBS/BPA (60/40, *W*/*W*) were selected for ^{1}H-NMR measurement (Fig. 1). The characteristic ^{1}H-NMR chemical shift for pure phenol hydroxyl locates at δ = 4.56. With the addition of PBS, the ^{1}H-NMR chemical shift of phenol hydroxyl shows a downfield shift, which is δ = 5.30 for PBS/BPA = 60/40. This result suggests that the interaction between PBS and BPA, *i.e.*, hydrogen bonding, is formed[30].

FTIR spectroscopy is another sensitive tool to characterize the hydrogen-bonding interaction, and is often used to probe the strong intermolecular interaction between phenol compounds and polymers containing carbonyl, ether or other functional groups[27–31]. Figure 2 shows the FTIR spectra of the PBS/BPA mixtures in the hydroxyl stretching vibration region. Pure PBS has a weak hydroxyl stretching vibration absorption at 3416 cm^{-1}. Pure BPA has a broad band with its peak at 3353 cm^{-1} and it is attributed to the hydroxyl stretching vibration absorption of self-H-bonded hydroxyl groups. In the PBS/BPA mixtures, the hydroxyl stretching vibration absorption band shifts to higher wavenumbers with the PBS content increasing. This peak shift is caused by the occurrence of intermolecular hydrogen bonds (inter-H-bonds) between PBS and BPA.

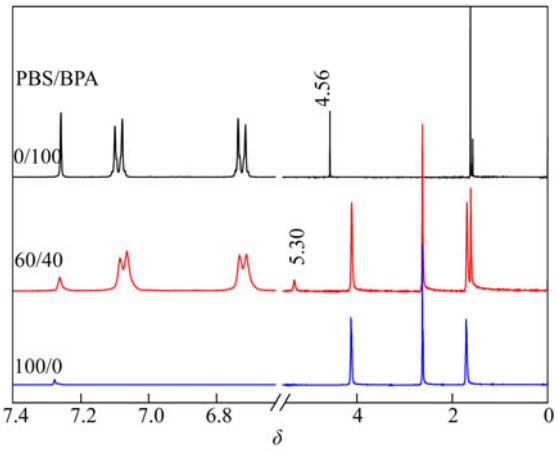

Fig. 1 ^{1}H-NMR spectra of pure PBS, BPA and their mixture (60/40, *W*/*W*)

Additionally, pure BPA has no IR absorption of the carbonyl group, so the variation of carbonyl group (C=O) band of PBS will be more helpful to illustrate the interaction between PBS and BPA. Figure 3 shows that the C=O stretching band of pure PBS has two absorption peaks at 1738 and 1722 cm^{-1}. Generally, crystalline polyesters have at least two absorption peaks in the region of C=O stretching band, originating from the C=O absorption of the crystalline component and amorphous component, respectively. For example, poly-(3-hydroxybutyrate-*co*-3-hydroxyvalerate) (PHBV) has two absorption peaks for the C=O stretching absorption. The one at higher wavenumbers (1740 cm^{-1}) corresponds to the amorphous component C=O absorption, and the other at lower wavenumbers (1723 cm^{-1}) is attributed to crystalline component C=O absorption[32]. For PBS, variable temperature FTIR experimental results (not given here for brevity) showed that the peak of 1738 cm^{-1} corresponds to the C=O absorption of PBS in the amorphous region, while the peak of 1722 cm^{-1} is ascribed to the C=O absorption of PBS in the crystalline region. For PBS/BPA mixtures, a new absorption peak at 1713 cm^{-1} emerges, the relative absorption intensity of which increases with BPA content. This peak is assigned to the hydrogen-bonding interaction between the C=O group of PBS and the OH group of BPA, resulting in red shift of C=O stretching band of PBS. At the same time, the benzene ring of phenol acts as an electron withdrawing group that holds the proton of a hydroxyl group less strongly[32]. All of these factors lead to the formation of intermolecular hydrogen bonds between the carbonyl groups of PBS and the hydroxyl groups of

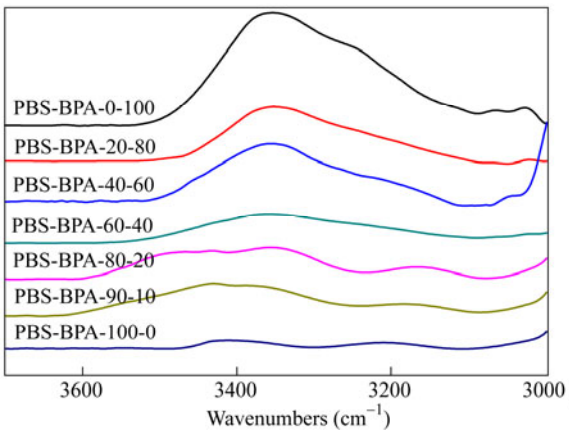

Fig. 2 FTIR spectra in hydroxyl stretching vibration regions of PBS/BPA mixtures

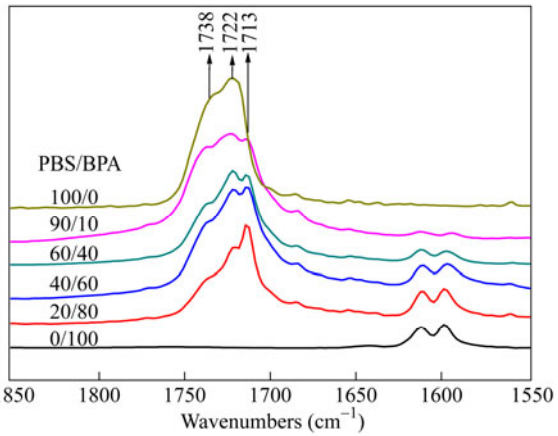

Fig. 3 FTIR spectra of pure PBS, BPA and their mixtures

BPA, resulting in the emerging of a new absorption peak at 1713 cm^{-1}. To quantitatively assess the fraction of the hydrogen-bonded carbonyl group in BPA, the integrated areas of amorphous (A_a), crystalline (A_c), and H-bonded (A_b) $\nu_{c=o}$ peaks of the mixtures were obtained by using a curve-fitting program. For example, the experimental and fitted spectra of PBS/BPA = 90/10 are illustrated in Fig. 4. The excellent agreement between the experimental and fitted spectra indicates the reliability of the curve-fitting technique. The relative fraction of the hydrogen-bonded, amorphous, and crystalline carbonyl groups in PBS are expressed by $A_b/(A_a + A_b + A_c)$, $A_a/(A_a + A_b + A_c)$, and $A_c/(A_a + A_b + A_c)$, respectively (Fig. 5). The relative fraction of hydrogen-bonded carbonyls notably increases with the BPA content, while that of the amorphous carbonyl groups and crystalline carbonyl groups decreases correspondingly.

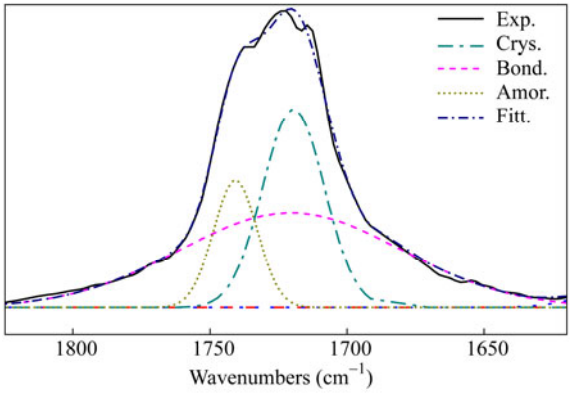

Fig. 4 Experimental and fitted FTIR spectra of the PBS/BPA = 90/10 blend
exp.: experimental spectrum; amor.: amorphous; crys.: crystalline; bond.: hydrogen-bonded component; fitt.: fitted spectrum, the sum of the amorphous, crystalline, and hydrogen-bonded components.

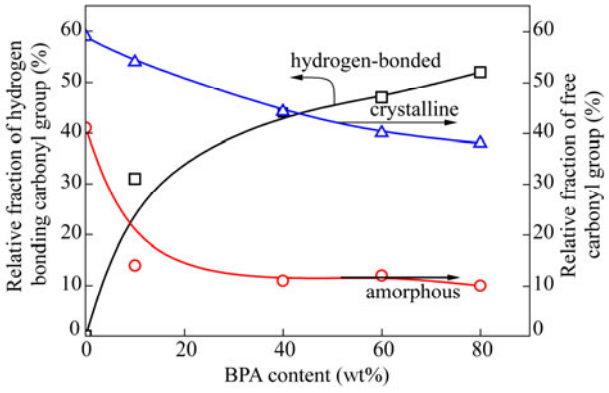

Fig. 5 Relative fraction of different carbonyl groups in PBS/BPA mixtures versus BPA content

Strong hydrogen-bond interactions can be formed between the ester groups and phenol hydroxyl groups in polymer mixtures at the expense of the self-association of phenol hydroxyls. The phenol hydroxyl group of BPA acts as the proton donor, while the carbonyl group of PBS plays the role of proton acceptor. Therefore, PBS associates with BPA *via* hydrogen-bonding interactions, leading to the construction of a cross-linking structure. It is expected that this cross-linking construction will confine the motion of the molecular chains of PBS in the mixtures, consequently increasing the T_g of PBS. The relationship between T_g and BPA content is depicted in Fig. 6. It is obvious that T_g increases linearly with BPA content. This result also suggests that PBS and BPA are miscible in the melting state[28]. By extrapolating the line to 100% BPA, the T_g of pure BPA is estimated to be 27.2 °C.

Crystallization Behavior of PBS/BPA Mixtures

Crystallization investigation on biodegradable polymers is important for understanding the condensed states of these materials. Figure 7 shows the interesting crystallization behavior of PBS/BPA mixtures. It was observed that the crystallization temperature (T_c) of PBS in the mixtures decreases with the increase of BPA content, from 71.7 °C for pure PBS to 42.6 °C for 80/20 (PBS/BPA) mixtures. The decrease of T_c of PBS in the mixtures indicates the formation of PBS-BPA supramolecular complexes, originating from the hydrogen-bonding interaction between the two components, which consequently suppresses the crystallization ability of the PBS. This suppression effect increases with BPA content. As BPA content exceeded 40%, DSC could not detect any crystallization peaks, indicating the crystallization ability of PBS is completely suppressed and a full amorphous eutectic mixture is formed[32]. In addition to pure BPA, no apparent crystallization peak of BPA in the mixtures can be detected on the DSC cooling curves, indicating that BPA in the PBS/BPA mixtures exists in a molecular

state[30]. This will be further confirmed by the following POM and WAXD experiments. The melting point of PBS in the mixtures was found, correspondingly, to decrease with increasing BPA content (Fig. 8). An obvious decrease of melting point of crystallizable components can be observed for almost all hydrogen-bonded mixtures[28, 33, 34]. For poly(*β*-hydroxybutyrate) (PHB)/poly(*p*-vinylphenol) (PVPh) blend, where a melting point decrease of 15 K was observed for PHB/PVPh=70/30 (wt%)[35]. The reduction in the melting temperature of PBS is caused by thermodynamic effects. When the two components in PBS/BPA mixtures are miscible and easy to interact through hydrogen bonding, the chemical potential of the crystallizable PBS decreases, leading to the decrease of the melting temperature[36, 37]. As BPA content is 40%, 60% or 80%, no melting peak of PBS can be detected due to amorphous eutectic mixture formation[32].

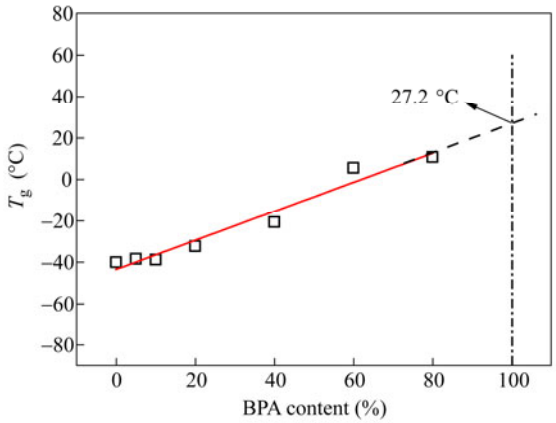

Fig. 6 Relationship between glass-transition temperature (T_g) of PBS and BPA content in PBS/BPA mixtures

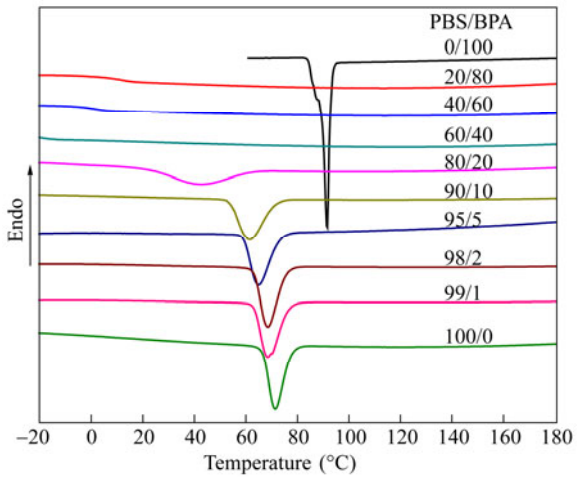

Fig. 7 DSC cooling curves of pure PBS, BPA and PBS/BPA mixtures at a cooling rate of 20 K/min

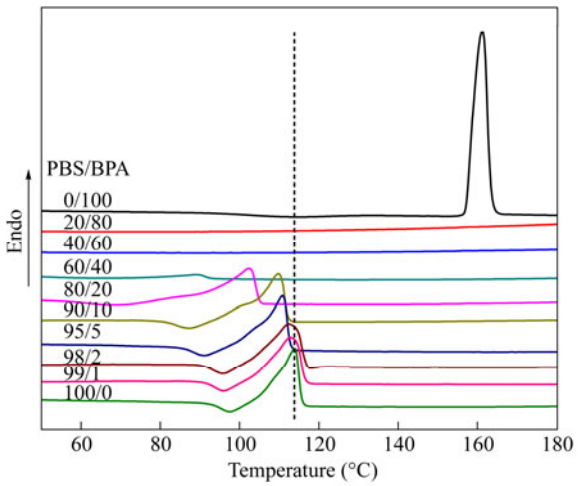

Fig. 8 DSC heating curves of pure PBS, BPA and PBS/BPA mixtures at a heating rate of 20 K/min

Although the non-isothermal crystallization process of polymers is close to the practical process, the samples crystallizing in this manner have a non-uniform inner structure and could not be used to explain the structural variation of the condensed state in the real forming process. So it is necessary to carry out crystallization experiments under isothermal conditions. According to Fig. 7, PBS is difficult to crystallize in mixtures with BPA content higher than 10%, therefore, the isothermal crystallization kinetics of PBS/BPA mixtures containing BPA of 0%, 2%, 5% and 10% was investigated. The relative crystallinity $X(t)$ of PBS was calculated according to the following equation:

$$X(t) = \frac{\int_0^t \frac{dH(t)}{dt} dt}{\int_0^{t_\infty} \frac{dH(t)}{dt} dt} = \frac{\Delta H_t}{\Delta H_\infty} \quad (1)$$

where the integral in the numerator is the heat generated at time t, and that in the denominator is the total heat generated in the whole crystallization process. Figure 9 shows the relative crystallinity X(t) as a function of time for pure PBS and PBS/BPA mixtures isothermally crystallized at 90 °C. The plots of crystallinity versus time are of *S* type, indicating that all the samples crystallize slowly at the early stage, and the crystallization processes accelerate at the middle stage, and then decrease again at the last stage. Similar results have also been observed for PBS/BPA mixtures at other crystallization temperatures of 86, 88 and 92 °C, which are not shown in this paper for brevity. In addition, it was also found that the formed hydrogen bonds suppress the crystallization of PBS, and this suppression effect increases with the fraction of the hydrogen-bonded carbonyl groups.

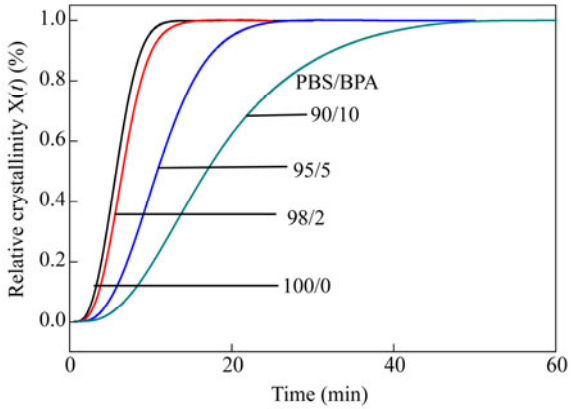

Fig. 9 Relative crystallinity of pure PBS and PBS/BPA mixtures as a function of time isothermally crystallized at 90 °C

The Avrami equation is an effective method for analyzing the isothermal crystallization kinetics of pure polymer and polymer mixtures. The equation is expressed as follows:

$$X(t) = 1 - \exp(-kt^n) \quad (2)$$

or

$$\lg[-\ln(1-X(t)] = n\lg t + \lg k \quad (3)$$

where n is the Avrami exponent depending on the nature of the nucleation and growth geometries of the crystals, and k is the overall crystallization rate constant involving both nucleation and growth rate parameters. The values of k and n can be calculated from the intercept and slope of Eq. (3). Figure 10 shows the relationship between lg[−ln(1−X(t)] and lg$t$ for pure PBS and PBS/BPA mixtures. A good linear relationship can be obtained for all the samples at the early crystallization stage. At the last crystallization stage, however, deviation can be observed for all the four samples. This is probably caused by the limitation of the Avrami method and the hydrogen-bonding effect. First, it is well known that the Avrami method is invalid for the last stage of crystallization due to the occurrence of secondary crystallization. On the other hand, the suppression effect of hydrogen bonds may partially destroy the perfection of PBS crystal and this influence is enhanced with the increase of BPA content. Hence, the deviation between theoretical and experimental occurs and increases with BPA content. The crystallization half time ($t_{1/2}$), which is defined as the time when X(t) reaches 50%, is an important parameter in the discussion of crystallization kinetics. The value of $t_{1/2}$ is directly obtained from Fig. 9. The related crystallization kinetics parameters n, k and $t_{1/2}$ for PBS and its mixtures are summarized in Table 1.

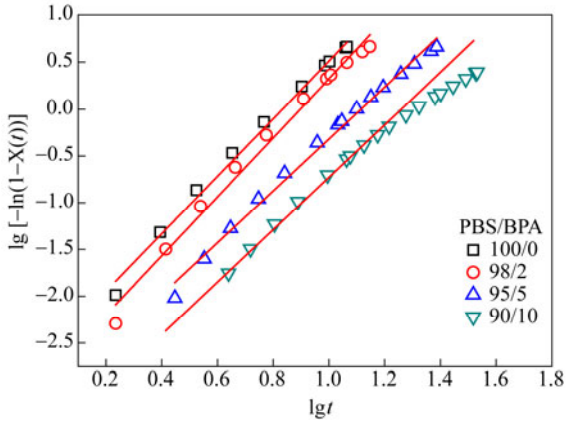

Fig. 10 Plot of lg[−ln(1−X(*t*))] versus lg*t* for pure PBS and PBS/BPA mixtures isothermally crystallized at 90 °C (symbols represent experimental data points, and solid lines represent fitted curves.)

Table 1. Crystallization kinetic parameters of pure PBS and PBS/BPA mixtures at different temperatures

PBS/BPA	T_c (°C)	n	k (min^{-n})	$t_{1/2}$ (min)
100/0	86	3.4	2.67×10^{-2}	2.6
	88	3.3	8.47×10^{-3}	3.7
	90	3.1	2.75×10^{-3}	5.9
	92	2.9	1.25×10^{-3}	9.0
98/2	86	3.4	2.27×10^{-2}	2.7
	88	3.2	6.90×10^{-3}	4.1
	90	3.1	1.48×10^{-3}	6.6
	92	2.9	6.48×10^{-4}	10.7
95/5	86	3.2	9.06×10^{-3}	3.8
	88	3.0	2.94×10^{-3}	6.2
	90	2.8	8.07×10^{-4}	10.7
	92	2.7	3.26×10^{-4}	16.5
90/10	86	3.0	4.56×10^{-3}	5.3
	88	2.9	1.23×10^{-3}	9.0
	90	2.8	3.08×10^{-4}	17.2
	92	2.7	1.31×10^{-4}	22.5

Table 1 shows that the values of n are non-integer in all cases, which may be a result of the mixed growth or surface nucleation[38]. The values of all n are around 3, indicating that PBS nucleates heterogeneously, regardless of the increase in crystallization temperature and the BPA contents. The values of $t_{1/2}$ are found to increase with the increase of crystallization temperature and the hydrogen-bond donor content. Generally, the crystallization rate is fancily described as the reciprocal of $t_{1/2}$. The values of $1/t_{1/2}$ and k decrease with increasing the hydrogen-bond donor content and crystallization temperature, indicating that crystallization is impeded by increasing crystallization temperature and hydrogen-bond donor content.

Spherulite Growth and Morphology of PBS and PBS/BPA Mixtures during Isothermal Crystallization Process

The spherulite growth rates of PBS in the mixtures were measured by using a polarizing optical microscope. The dependence of spherulite growth rate (G) on T_c for pure PBS and different PBS mixtures is shown in Fig. 11, indicating that the spherulite growth rates decrease with increasing crystallization temperature and BPA content. The above results suggest that the formed hydrogen bonds between PBS and BPA significantly impede the spherulite growth rate of PBS in the mixtures. The suppression effect of the hydrogen bonds on spherulite growth rate at lower crystallization temperature is more obvious. The crystallization rate decrease of PBS in mixtures are caused by: (1) the decrease in segmental mobility of the crystalline polymer transporting across the liquid-solid interface because of the high T_g of the PBS/BPA mixtures, (2) the decrease of thermodynamic

driving force of the growth of PBS spherulites due to the decrease in T_m in the mixtures and (3) the diluent effect reducing the number of crystalline chain segment at the surface of the growth spherulites[38, 39].

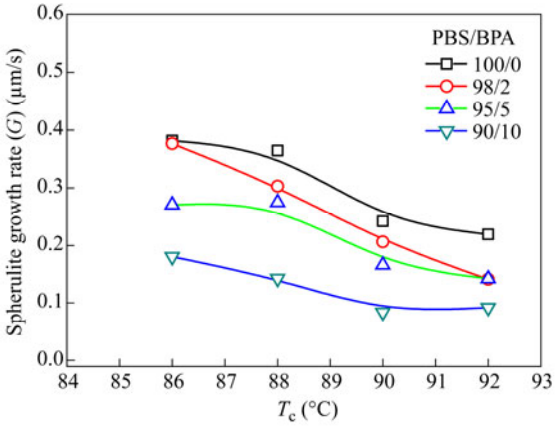

Fig. 11 Spherulite growth rates (G) as a function of T_c for pure PBS and PBS/BPA mixtures

Figure 12 shows the spherulite morphology of PBS and its mixtures isothermally crystallized at 92 °C. The spherulites of pure PBS are compact. In the case of the PBS/BPA mixtures, the PBS spherulites become coarse compared with those of pure PBS. The size of the spherulite increases with BPA content, which is caused by the dilute effect and the decrease in supercooling degree resulting from the decrease in melting point of PBS in the mixtures. For pure PBS, most of the boundaries between two spherulites are bent. With the addition of BPA,

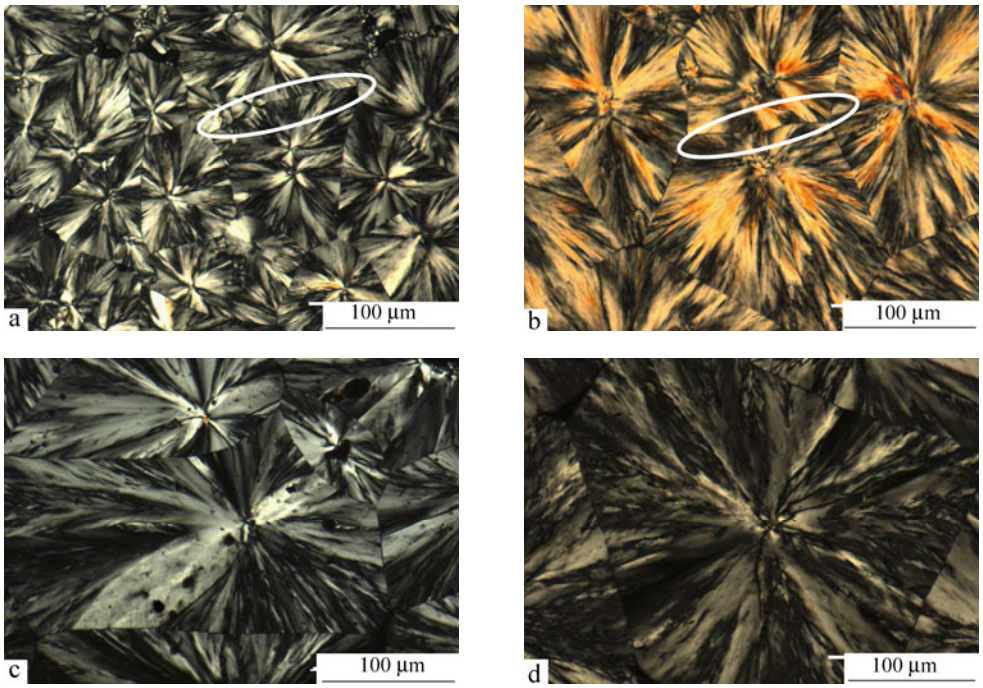

Fig. 12 Spherulite morphology of pure PBS and PBS/BPA mixtures crystallized at 92 °C: (a) pure PBS, (b) PBS/BPA = 98/2, (c) PBS/BPA = 95/5 and (d) PBS/BPA = 90/10 (White circle in (a) represents bent boundary and that in (b) represents planar boundary)

the bent boundary partially changed into planar, suggesting that the probability of spherulite crystallized at the same time increases with the BPA content[40]. The spherulites of pure and blended PBS are space filling, indicating that PBS-BPA hydrogen-bonding associated components are rejected during the crystallization process as non-crystallizable components, residing primarily in the interlamellar and/or interfibrillar domains of the PBS spherulites[41, 42]. Figure 13 shows the WAXD patterns of pure and PBS/BPA mixtures. Both the pure and mixed PBS exhibit the same diffraction peaks at the same locations, indicating that blending with BPA does not modify the crystal structure of PBS, and BPA is excluded from the crystal region of PBS and exists in the amorphous region. The three main peaks locating at around 19.4°, 21.9° and 22.6° correspond to the planes of (020), (021) and (110), respectively. Based on the above analysis, a schematic diagram is proposed for the PBS-BPA inter-associated existence region in the PBS/BPA mixtures (Fig. 14). The phenol hydroxyl group associates with carbonyl group in PBS chain to form supramolecular complex by hydrogen-bonding. The complex of PBS-BPA exists in the amorphous region.

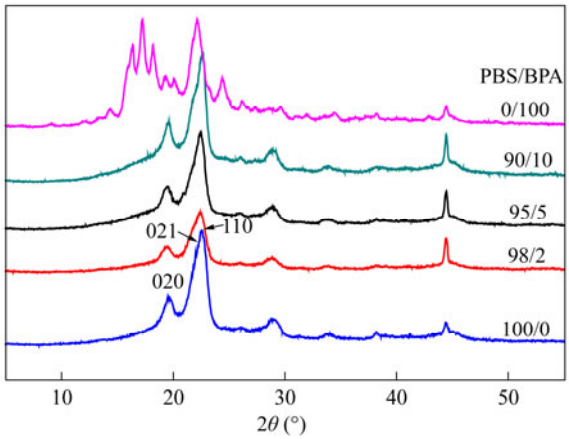

Fig. 13 WAXD patterns of pure PBS and PBS/BPA mixtures

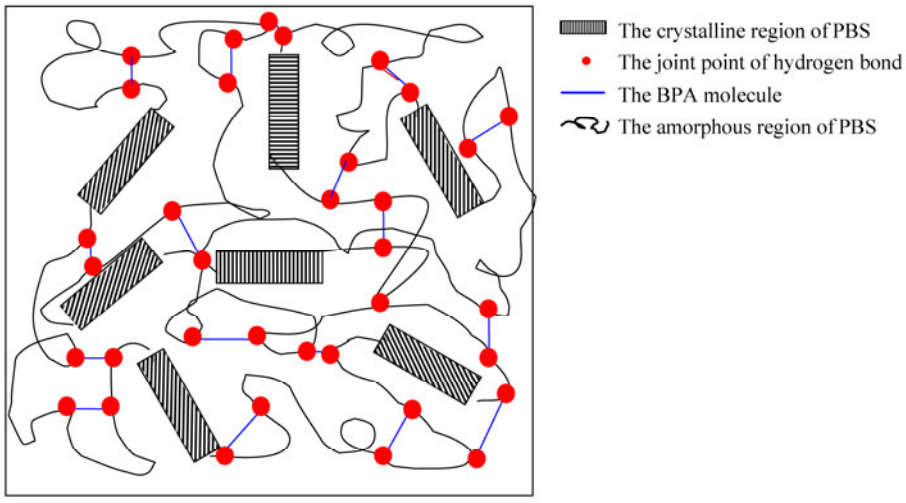

Fig. 14 Schematic illustration of the PBS-BPA inter-associated existence in the mixtures

CONCLUSIONS

The intermolecular interaction and crystallization behavior of PBS/BPA mixtures were investigated by the combination of NMR, FTIR, DSC, POM and WAXD, and following conclusions are obtained:

(1) In PBS/BPA mixtures, intermolecular hydrogen bonds are formed between the carbonyl groups of PBS

and the hydroxyl groups of BPA. The fraction of hydrogen-bonded carbonyl group increases with BPA content.

(2) The crystallization temperature of PBS in PBS/BPA mixtures decreases with the increase of BPA content during non-isothermal crystallization process, and the melting point of PBS in the mixtures decreases with the increase of BPA content. When the hydrogen-bond donor (BPA) exceeds 40% in the mixtures, PBS will not crystallize and no melting point of PBS can be observed.

(3) In the process of isothermal crystallization, PBS crystallizes with heterogeneous nucleation, regardless of the increase of crystallization temperature and the BPA content. The crystallization kinetics and spherulite morphology of PBS are apparently influenced by both crystallization temperature and hydrogen-bond donor. The overall crystallization rates decrease with the increase of crystallization temperature and BPA content.

REFERENCES

1 Lai, S.M., Huang, C.K. and Shen, H.F., J. Appl. Polm. Sci., 2005, 97: 257
2 Lee, S.M., Cho, D., Park, W.H., Lee, S.G., Han, S.O. and Drzal, L.T., Compos. Sci. Technol., 2005, 65: 647
3 He, Y., Zhu, B., Kai, W. and Inoue, Y., Macromolecules, 2004, 37: 3337
4 Qiu, Z.B., Ikehara, T. and Nishi, T., Polymer, 2003, 44: 3095
5 Wang, H.J., Schultz, J.M. and Yan S.K., Polymer, 2007, 48: 3530
6 Qiu, Z.B., Ikehara, T. and Nishi, T., Polymer, 2003, 44: 2503
7 Qiu, Z.B., Komura, M., Ikehara, T. and Nishi, T., Polymer, 2003, 44: 8111
8 Wang, T.C., Li, H.H., Yan, S.K., Chinese J. Polym. Sci., 2012, 30(2): 269
9 Li, Y.J., Kaito, A. and Horiuchi, S., Macromolecules, 2004, 37: 2119
10 Qiu, Z.B., Yan, C.Z., Lu, J.M., Yang, W.T., Ikehara, T. and Nishi, T., J. Phys. Chem. B, 2007, 111: 2783
11 Wang, H.J., Gan, Z H., Schultz, J.M. and Yan, S.K., Polymer, 2008, 49: 2342
12 Ikehara, T., Kurihara, H., Qiu, Z.B. and Nishi, T., Macromolecules, 2007, 40: 8726
13 Qiu, Z.B., Ikehara, T. and Nishi, T., Polymer, 2003, 44: 2799
14 Qiu, Z.B., Ikehara, T. and Nishi, T., Polymer, 2003, 44: 7519
15 Qiu, Z.B., Komura, M., Ikehara, T. and Nishi, T., Polymer, 2003, 44: 7749
16 Qiu, Z.B. and Yang, W.T., Polymer, 2006, 47: 6429
17 Hwang, S.Y., Yoon, W.J., Yoo, E.S. and Im, S.S., Macromol. Res., 2012, 20: 1088
18 Shih, Y.F., Chen, L.S. and Jeng, R.J., Polymer, 2008, 49:4602
19 Ray, S.S., Vaudreuil, S., Maazouz, A. and Bousmina, M., J. Nanosci. Nanotechnol., 2006, 6: 2191
20 Song, L. and Qiu, Z.B., Polym. Degrad. Stab., 2009, 94: 632
21 Song, L.and Qiu, Z.B., J. Nanosci. Nanotechnol., 2010, 10: 965
22 Lv, S.G., Plastics Additives Handbook, first edition, Light Industry Press: Beijing, 1988, p. 51; 903; 427; 453
23 Cai, Y.L., Wang, D.J., Hu, X.B., Xu, Y.Z., Zhao, Y., Wu, J.G. and Xu, D.F., Macromol. Chem. Phys., 2001, 202: 2434
24 Yu, T., Zhou, Y., Zhao, Y., Liu, K P., Chen, E.Q., Wang, D.J. and Wang, F.S., Macromolecules, 2008, 41: 3175
25 Zhou, S.R., Shi, H.F., Zhao, Y., Jiang, S.C., Lu,Y.L., Cai, Y.L., Wang, D.J., Han, C.C. and Xu, D.F., Macromol. Rapid Commun., 2005, 26: 226
26 Zhou, S.R., Zhao,Y., Cai, Y.L., Wang, D.J. and Xu, D.F., Chem. Commun., 2003, 15: 1932
27 Wu, C., J. Appl. Polym. Sci., 2001, 80: 2468
28 He, Y., Asakawa, N., Li, J.C. and Inoue, Y., J. Appl. Polym. Sci., 2001, 82: 640
29 He, Y., Asakawa, N. and Inoue, Y., J. Polym. Sci. Part. B: Polym. Phys., 2000, 38: 1848
30 Fei, B., Chen, C., Wu, H., Pen, S.W., Wang, X.Y., Dong, L.S. and Xin, J.H., Polymer, 2004, 45: 6275
31 He, Y., Asakawa, N. and Inoue, Y., Macromol. Chem. Phys., 2001, 202: 1035
32 Li, J.C., Fukuoka, T., He, Y., Uyama, H., Kobayashi, S. and Inoue, Y., J. Appl. Polym. Sci., 2005, 97: 2439
33 Li, J.C., He, Y., Ishida, K., Yamane, T. and Inoue, Y., Polym. J., 2001, 33: 773
34 He, Y., Asakawa, N. and Inoue, Y., J. Polym. Sci. Part B: Polym. Phys., 2000, 38: 2891

35 Xing, P.X., Dong, L.S., An, Y.X., Feng, Z.L. Avella, M. and Martuscelli, E., Macromolecules, 1997, 30: 2726
36 Kuo, S.W., J. Polym. Res., 2008, 15: 459
37 He, Y., Zhu, B. and Inoue, Y., Prog. Polym. Sci., 2004, 29: 1021
38 Kuo, S.W., Chan, S.C. and Chang, F.C., Macromolecules, 2003, 36: 6653
39 Lu, J.M., Qiu, Z.B. and Yang, W.T., Macromol. Mater. Eng., 2008, 293: 930
40 StÖbl, G., The Physics of Polymers, The Semicrystalline State, third edition, Heidelberg: Springer-Verlag, Berlin, 2007, p. 172
41 Keith, H.D. and Padden, F.J., J. Appl. Phys., 1964, 35: 1286
42 Keith, H.D. and Padden, F.J., J. Appl. Phys., 1964, 35: 1270